

# A computational study on power-law rheology of soft glassy materials with application to cell mechanics

A. Vaziri <sup>a</sup>, Z. Xue <sup>a</sup>, R.D. Kamm <sup>b</sup>, M.R. Kaazempur Mofrad <sup>c,\*</sup>

<sup>a</sup> School of Engineering and Applied Sciences, Harvard University, Cambridge, MA 02138, United States

<sup>b</sup> Department of Mechanical Engineering and Biological Engineering Division, Massachusetts Institute of Technology, Cambridge, MA, United States

<sup>c</sup> Molecular Cell Biomechanics Laboratory, Department of Bioengineering, University of California, Berkeley, CA 94720, United States

Received 13 February 2006; received in revised form 27 June 2006; accepted 28 November 2006

---

## Abstract

Response of the cytoskeleton to mechanical stimulus, which involves coordinated assembly and disassembly of cytoskeletal polymers and their coupling to motor proteins, has been shown to be governed by a ubiquitous mechanical behavior called power-law rheology. Various experimental techniques in cell mechanics have yielded similar qualitative observations and quantitative behavior indicating that the power-law rheology is an intrinsic feature of the cell structure. In this study, a biomechanical model of the cell in microbead twisting experiments is developed which incorporates the material law associated with power-law rheology using the finite element method. Such a biomechanical model can help elucidating the mechanics of cytoskeletal responses and relate the microrheology of the cytoskeleton to its overall behavior under mechanical stimulus. This biomechanical model is employed to explore the role of material constants associated with power-law rheology on the overall response of a cell in magnetic twisting cytometry. Furthermore, the computational approach is employed to mimic the experimental observations of [B. Fabry, G.N. Maksym, J.P. Butler, M. Glogauer, D. Navajas, J.J. Fredberg, Scaling the microrheology of living cells, *Phys. Rev. Lett.* 87 (2001) 148102; B. Fabry, G.N. Maksym, J.P. Butler, M. Glogauer, D. Navajas, N.A. Taback, E.J. Millet, J.J. Fredberg, Time scale and other invariants of integrative mechanical behavior in living cell, *Phys. Rev. E*, 68(4) (2003) 041914] on living cells.

© 2007 Published by Elsevier B.V.

**Keywords:** Cytoskeletal mechanics and rheology; Power-law rheology; Soft glassy materials

---

## 1. Introduction

Numerous biological processes are influenced by mechanical stimulation, making the rheological properties of living cells critical to their function. Recent experiments, carried out over a range of length scales using different methods, have shed light on dynamic responses of the cytoskeleton to mechanical perturbation [2–10]. These experiments indicate that the cell response over a broad frequency spectrum is governed by a ubiquitous mechanical behavior called power-law rheology which is an intrinsic feature of many soft materials such as emulsions, pastes, foams and colloids [11–15]. These materials which all fall in

the category of soft glassy materials are composed of numerous discrete elements that experience weak interactions with inherently disordered and metastable microstructural geometry. The complex dynamics exhibited by these materials, which exists far from thermodynamic equilibrium, exhibits power-law frequency dependence with no single characteristic frequency or timescale. The material law in the frequency domain for soft glassy rheology, in which the storage and loss moduli depend on the excitation frequency with the same power exponent and have a constant ratio, is in the form of

$$\begin{aligned} G'(\omega) &= G_0(\omega/\omega_0)^{x-1} \cos \left[ \frac{(x-1)\pi}{2} \right], \\ G''(\omega) &= G_0(\omega/\omega_0)^{x-1} \sin \left[ \frac{(x-1)\pi}{2} \right], \end{aligned} \quad 1 \leq x \leq 2, \quad (1)$$

---

\* Corresponding author.

E-mail address: [mofrad@berkeley.edu](mailto:mofrad@berkeley.edu) (M.R. Kaazempur Mofrad).

where  $G'(\omega)$  and  $G''(\omega)$  are the frequency-dependant shear storage and loss moduli of the material, respectively,  $\omega$  is the radian frequency of excitation and  $x$  is identified as being the ‘noise temperature’.  $G_0$  denotes the shear storage modulus of the material at the glass transition ( $x = 1$ ) and  $\omega_0$  is the reference frequency. This material law also can be represented in the form of

$$\begin{aligned} G'(\omega) &= G_0(\omega/\omega_0)^{x-1} \cos\left[\frac{(x-1)\pi}{2}\right], \\ G''(\omega) &= \eta G'(\omega), \end{aligned} \quad 1 \leq x < 2, \quad (2)$$

where  $\eta = G''(\omega)/G'(\omega) = \tan((x-1)\pi/2)$  is the structural damping coefficient. The physical interpretation of each of the material constants associated with power-law rheology is discussed in [1]. It is noteworthy that in Sollich’s theory [1,16], a characteristic reference frequency is considered as the maximum rate at which material elements can escape their traps. Insight into the mechanistic basis of cytoskeleton rheology is provided in [17,18], where the role of contractile stresses in the cytoskeleton on regulating its rheological properties was explored.

Computational models that incorporate the material law associated with power-law rheology can help to describe the overall response of the material, providing a tool for accurate assessment of the material constants associated with the power-law rheology from experimental observations. Lau et al. [19] showed that the cytoskeleton can be treated as a coarse-grained continuum with power-law rheology, driven by a spatially random stress tensor field. Here, we develop a computational approach incorporating a power-law material model based on finite element method and employ it to explore cytoskeleton dynamics by simulating the cell response in twisting bead experiments as described in [2,3]. The theoretical background of the material model is presented in Section 2, while the details of the computational model are described in Section 3. A parametric study is carried out in Section 4 using the developed computational model. In Section 5, the developed computational model is employed to replicate experimental measurements on human airway smooth muscle (HASM) cells from Fabry et al. [3]. Conclusions from the computations are presented in Section 6.

## 2. Theoretical background

To model the frequency dependence exhibited by soft glassy materials, we adopted the frequency-domain viscosity model, in conjunction with isotropic linear elasticity [20]. Consider a shear test at small strain, in which a harmonically varying shear strain of amplitude  $\gamma_0$  and radian frequency  $\omega$  is applied

$$\gamma(t) = \gamma_0 e^{i\omega t}, \quad (3)$$

where  $i = \sqrt{-1}$  and  $t$  is time. We consider the situation in which the specimen has been exposed to oscillatory forcing for a very long time so that a steady-state response is

achieved. The solution for the shear stress then has the form

$$\tau(t) = G(\omega)\gamma_0 e^{i\omega t}, \quad (4)$$

where  $G(\omega)$  is the complex, frequency-dependent shear modulus of the material and is in the form of

$$G(\omega) = G'(\omega) + iG''(\omega). \quad (5)$$

Eq. (3) implies that the material response to applied harmonic strain is the superposition of a stress of magnitude  $G'(\omega)\gamma_0$  that is in phase with the strain and a stress of magnitude  $G''(\omega)\gamma_0$  that lags the excitation by  $90^\circ$ . The absolute magnitude of the stress amplitude is

$$|\tau_0| = \sqrt{G'^2(\omega) + G''^2(\omega)}\gamma_0 \quad (6)$$

and the associated phase lag of the stress response is

$$\phi = \arctan\left(\frac{G''(\omega)}{G'(\omega)}\right). \quad (7)$$

Experimental measurements of  $|\tau_0|$  and  $\phi$  at various excitation frequencies can thus be used to estimate  $G'(\omega)$  and  $G''(\omega)$ . In the subsequent calculations, we consider the material model associated with power-law rheology, where the storage and loss moduli both vary as  $\omega^{x-1}$  with a constant, frequency-independent ratio as expressed in Eq. (1). The developed computational approach is capable of incorporating other types of frequency-dependant rheologies (as will be exemplified later).

The employed constitutive law assumes that the shear (deviatoric) and volumetric behaviors are independent in multiaxial stress states. Similar to that for shear, a complex, frequency-dependent bulk stiffness, in the form of  $K(\omega) = K'(\omega) + iK''(\omega)$ , can be incorporated in the calculations. However, for the present application, we have simply treated the bulk modulus as real and constant:  $K'(\omega) = K = \text{constant}$  and  $K''(\omega) = 0$ , and postulated that the viscous behavior of cell is associated only with deviatoric straining. The bulk modulus is related to the material elastic modulus,  $E$ , and Poisson ratio,  $\nu$ , which are the input to the finite element model, by:  $K = E/3(1 - 2\nu)$ .

## 3. Details of the computational model

Numerical simulations were performed corresponding to published experiments using the method of magnetic twisting cytometry (MTC) that has been widely employed for the measurement of cell rheology (Fig. 1). In all the calculations, the microbead is modeled as a rigid sphere with radius  $2.25 \mu\text{m}$ . The material bonded to the rigid sphere is taken to be homogeneous and isotropic with density  $\rho$  and follow the material model associated with power-law rheology under shear, while its volumetric behavior is assumed to follow a linear elastic response (as described in Section 2). The bottom surface of the substrate is fixed while other surfaces are unconstrained (zero stress). To minimize the effect of boundary conditions, the model dimensions are

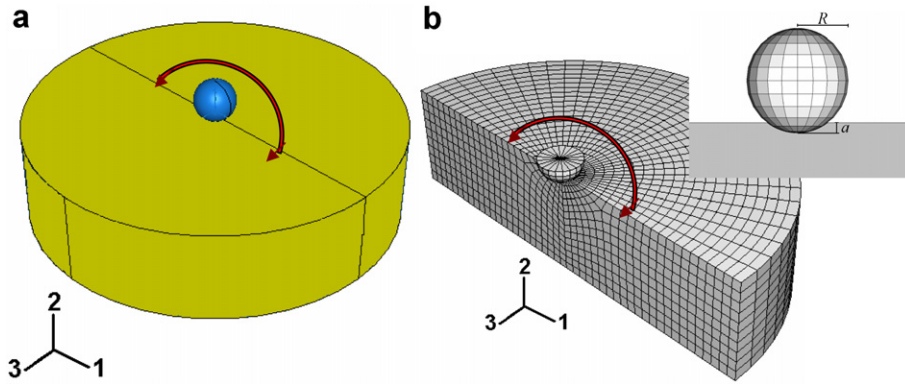


Fig. 1. (a) Schematic diagram of magnetic twisting cytometry. (b) Corresponding computational model. Only one half of the system is analyzed due to the symmetry of the structure and the loading conditions as shown in the computational model. The arrows show the direction of the applied harmonic torque (along axis 3). Eight-node linear brick elements with reduced integration are used in the calculations (C3D8R) [20]. The microbead is modeled as a rigid sphere (inset).

taken to be substantially larger than the microbead radius and the induced-displacement field. The microbead is fully bonded to the material and is constrained to undergo translation only in the direction of axis 1 and rotation along axis 3 (see Fig. 1). A harmonic excitation in the form of  $T(t) = T_0 e^{i\omega t}$  with frequency of  $f = \omega/2\pi$  is applied to the microbead. The frequency-domain viscosity model, discussed in Section 2, is employed in the computations to study the steady-state response of the cytoskeleton. The frequency-dependant shear storage and loss moduli are inputted to the computational model for each set of material constants associated with power-law rheology,  $G_0$ ,  $\omega$  and  $\omega_0$ . The steady-state linearized response of the system is attained by performing direct-solution steady-state dynamic analysis [20]. All computations are performed using a commercially available finite element modeling software ABAQUS (Hibbit, Karlsson and Sorensen Inc., Providence, RI). To accurately capture details of deformation and the associated stress/strain patterns, a finer mesh pattern is employed in the vicinity of the microbead. A mesh sensitivity study was conducted to ensure the independence of the results from the computational mesh to within 1% in bead motion. In these calculations, we neglect the effect of pre-stress in the surrounding material due to inserting the microbead. Although this can be incorporated in the constitutive behavior, we hypothesized that the harmonic excitation is applied sufficiently long after the microbead attachment so that the surrounding material has had time to remodel and thereby relax any stresses this initial deformation might impose. The output of these computational analyses includes the steady-state displacement amplitude and phase angle at nodal points including the nodal point associated with the rigid microbead.

It should be emphasized that although the developed computational model is capable of analyzing the response of the material with power-law rheology under steady-state dynamic loading, however it can not be directly employed for other loading conditions such as quasi-static and transient loading conditions. While MTC is the most widely used method for characterizing the rheology of cytoskele-

ton, however other experimental procedures such as micropipette aspiration have recently yielded similar qualitative observations indicating that the power-law rheology is an intrinsic feature of the cell structure. This motivates developing computational approaches for analyzing the response of these materials under general loading conditions, which is the focus of our future study.

#### 4. Numerical results

Results are presented in terms of time histories of applied harmonic torque and the corresponding steady-state response of the microbead (Fig. 2a). The bead movement lags the imposed harmonic force/torque, which is the intrinsic characteristic of systems with viscosity. The viscoelastic material model presented in Eq. (1) has three independent material constants,  $(G_0, \omega_0, x)$ . In all the calculations presented in this section, the following parameters are set to be constant:  $\rho = 1 \text{ g/cm}^3$ ,  $E = 2.9 \text{ kPa}$ ,  $\nu = 0.45$  (which corresponds to the bulk modulus of  $K = 9.7 \text{ kPa}$ ,  $G_0 = 1 \text{ kPa}$ ,  $\omega_0 = 1 \text{ rad/s}$ ). In this study, we kept the material Poisson ratio constant ( $\nu = 0.45$ ) to focus our study on the role of material constants associated with the power-law rheology on the response. However, a set of calculations was carried out to study the role of material bulk modulus, which characterizes its volumetric behavior, on the response under harmonic excitation applied to the microbead for a constant set of material constants associated with the power-law rheology. The results reveal a considerable sensitivity of the response amplitude to the material bulk modulus but little qualitative difference. The degree of sensitivity depends on the excitation frequency and  $x$  (data not shown).

Fig. 2b and c show the calculated torque–displacement response at various frequencies of applied excitation for material having  $x = 1.2$  (corresponding to  $\eta = 0.325$ ) and  $x = 1.5$  (corresponding to  $\eta = 1$ ), respectively. The amplitude of the response decreases with increasing frequency of applied excitation leading to a more localized deformation. Distributions of the amplitude of effective (von Mises)

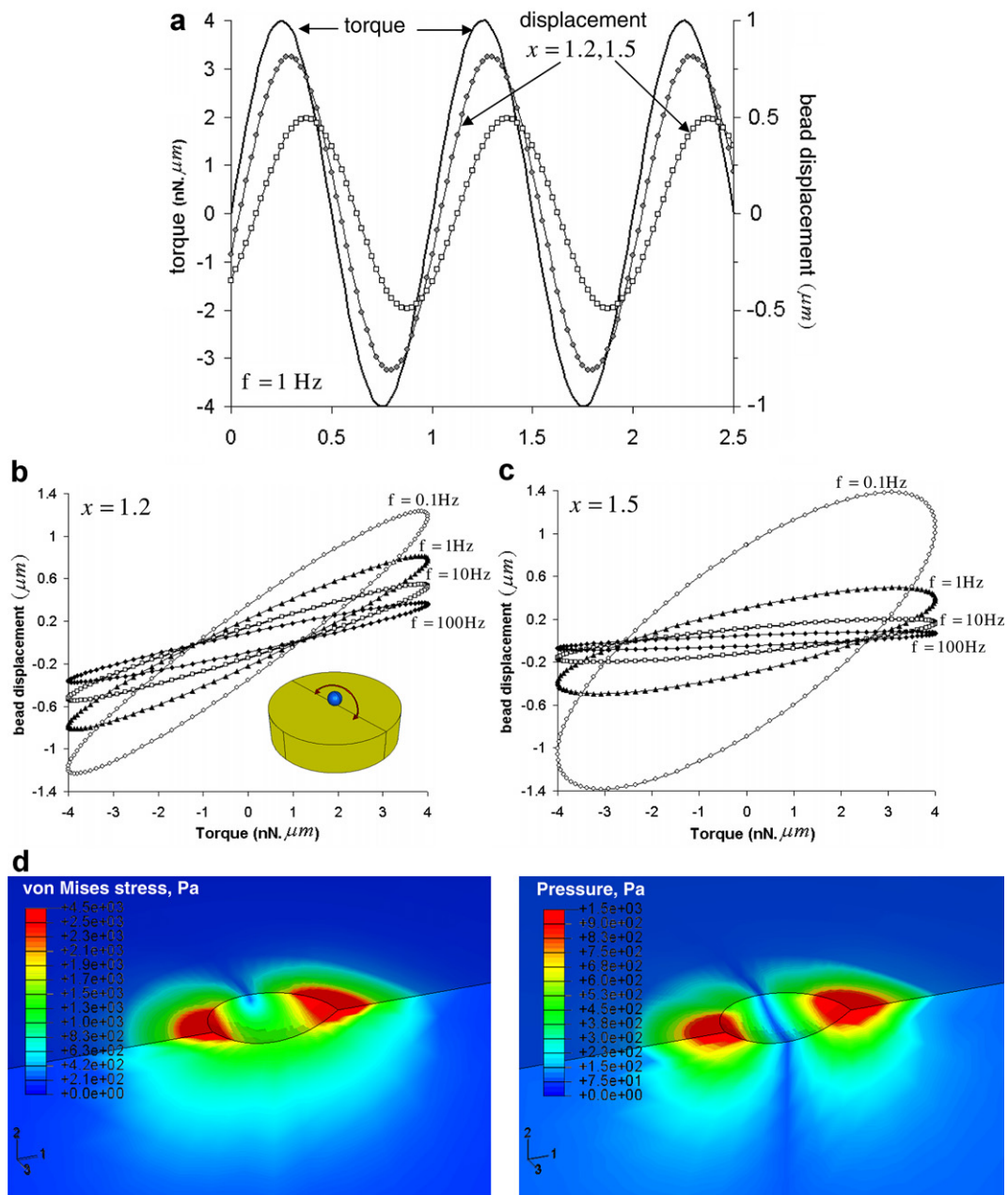


Fig. 2. (a) Time histories of applied harmonic excitation and displacement of the center of the microbead along axis 1 at the excitation frequency of 1 Hz for  $x = 1.2$  (corresponding to  $\eta = 0.325$ ) and  $x = 1.5$  (corresponding to  $\eta = 1$ ). (b) and (c) Simulated torque–displacement response in MTC at various frequencies of harmonic torque for  $x = 1.2$  and  $x = 1.5$ , respectively. The phase angle between torque and bead displacement remain approximately constant for each set of calculations and only depends on  $x$  ( $\sim 15^\circ$  for  $x = 1.2$  and  $\sim 45^\circ$  for  $x = 1.5$ ). (d) Distributions of the amplitude of effective (von Mises) stress and amplitude of pressure for  $x = 1.5$  and  $f = 1$  Hz. (The calculated pattern is not fully symmetric with respect to the 2–3 plane crossing the center of the bead due to numerical error.) The results are presented for the following parameter values:  $G_0 = 1$  kPa,  $\omega_0 = 1$  rad/s,  $E = 2.9$  kPa,  $\rho = 1$  g/cm<sup>3</sup>,  $\nu = 0.45$ . The rigid microbead has a radius  $R = 2.25$   $\mu$ m with  $a/R = 0.178$ . A harmonic torque with the amplitude of  $T_0 = 4$  nN  $\mu$ m is applied along axis 3.

stress and hydrostatic pressure in the model with  $x = 1.5$  excited at the frequency of 1 Hz are depicted in Fig. 2d. The dependence of the amplitude of bead displacement on the excitation frequency is depicted in Fig. 3 in log–log scale for various values of  $x$  ranging between  $1 \leq x \leq 2$ . It is noteworthy that at the glass transition, i.e.  $x = 1$ , the material properties are independent of the frequency of excitation, i.e.  $G' = G_0$  while  $G'' = 0$ . At high

frequencies of excitation, the amplitude of response substantially decreases on increasing the value of  $x$  (Fig. 3b). In contrast at low frequencies of excitation, the amplitude of response increases on increasing the value of  $x$  from 1. The distribution of the amplitude of effective stress and amplitude of hydrostatic pressure in general exhibit a significantly lower sensitivity to the excitation frequency and material constant  $x$  (data not shown).

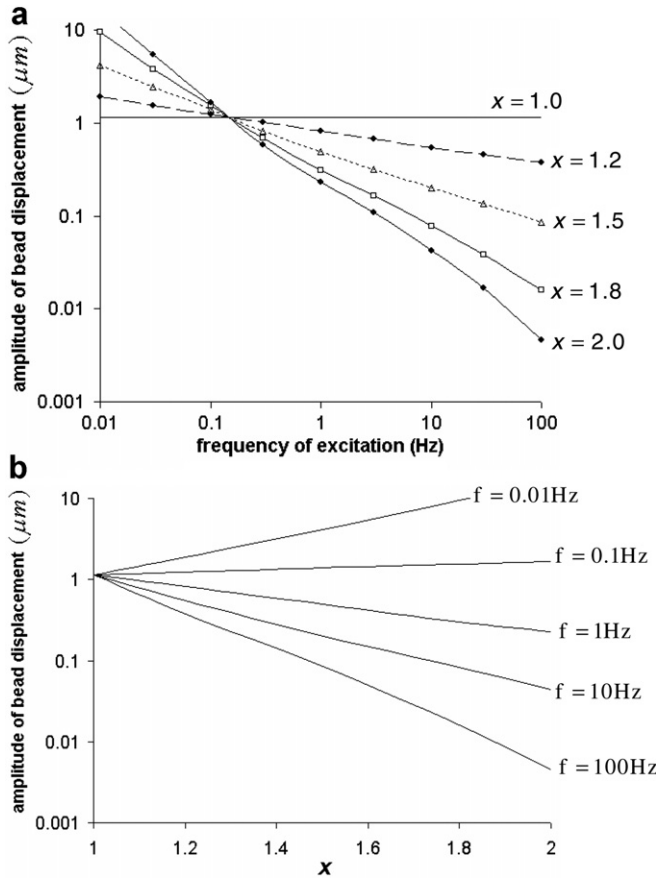


Fig. 3. (a) Dependence of the response amplitude (displacement along axis 1) on the frequency of excitation for various values of  $x$ . (b) Dependence of the response amplitude on  $x$  at various excitation frequencies. Calculations are performed using:  $G_0 = 1$  kPa,  $\omega_0 = 1$  rad/s,  $E = 2.9$  kPa,  $\rho = 1$  g/cm<sup>3</sup>,  $\nu = 0.45$ . The rigid microbead has a radius  $R = 2.25$   $\mu$ m with  $a/R = 0.178$ . Amplitude of the applied torque is  $T_0 = 4$  nN  $\mu$ m.

In the numerical study presented here and in interpreting the experimental observations, which will be discussed in Section 5, the cell is modeled as one homogenous isotropic material, neglecting the roles of the membrane, cortex or nucleus. This is in agreement with a similar computational model by Mijailovich et al. [21], where the cytoskeleton is assumed to be a homogeneous linear elastic material. Our previous studies show that the role of the cell membrane on the overall response of cell during magnetocytometry is negligible at low to moderate frequencies ( $\sim 100$  Hz) [22]. However, it is conceivable that the cell membrane could significantly alter the mechanical response and its underlying mechanisms at higher frequencies or under different loading conditions such as indentation [23], emphasizing the need for biomechanical models of the cell that incorporate these different structures.

## 5. Comparison with experimental observations

The proposed computational model for magnetic twisting cytometry (MTC) is employed to mimic the experimental observations of Fabry et al. [3] on HASM cells. The

experiments were performed using MTC with optical detection of bead motion [24,25]. The ferromagnetic microbeads were coated with a variety of antibody and non-antibody ligands, which bind to specific cell surface receptors that link to the cytoskeleton (e.g., via integrin receptors). This is consistent with the assumption of no-slip, no-separation contact in our numerical simulations. The readers are referred to Fabry et al. [3] for details of cell culture and experimental procedure. Analysis of the experimental data clearly indicates that the cytoskeleton behaves according to power-law rheology with parameter  $x$ , which is defined as material ‘noise temperature’ in Sollich’s theory [1,16], lying between 1.15 and 1.35 for various cell types with the value of  $\sim 1.2$  for HASM cells [2,3]. Another interesting point that emerges from the experimental measurements is that for all practical purposes a single parameter  $x$  is sufficient to characterize the changes in cell material behavior under various forms of drug-induced challenges to the cell, namely contraction or relaxation of the cytoskeletal network [2,3,13,15], since  $G_0$  and  $\omega_0$  appear to be universal constants. One intriguing aspect of the experimental results is the degree of variability observed when the bead is tethered to different receptors, or, even when beads of different composition are coated with the same ligand [10]. This raises the prospect that receptor-ligand binding kinetics, or more specifically, the character of bond formation and rupture, might influence experimental results for membrane-tethered microbeads. While the observed agreement of intracellular bead motion to power-law rheology in other recent experiments on isolated nuclei [26] suggests that receptor kinetics are not dominant, similar effects throughout the cytoskeleton, involving, for example, transient binding and rupture of actin cross-linking proteins, could contribute to the overall behavior.

Here, fitting to the experimental results is achieved by varying  $G_0$  and  $x$ , while the following material properties are prescribed in the computations;  $\rho = 1$  g/cm<sup>3</sup> and  $\nu = 0.45$ . To further limit the number of material parameters in the fitting procedure, in this set of calculations we assumed that the ratio of the material bulk modulus to its shear storage modulus at the reference excitation frequency of 1 rad/s, i.e.  $G_0/K$ , remains constant and equal to 0.1. It was found that the computational results closely replicate the experimental observations for the following material constants associated with power-law rheology:  $G_0 = 3.8$  kPa for  $\omega_0 = 1$  rad/s and  $x = 1.3$  (corresponding to  $\eta \simeq 0.51$ ) (Fig. 4). The fitting to the experimental results using our computational model suggests a slightly stronger frequency-dependence than that reported in Fabry et al. [3] ( $x \sim 1.2$  for HASM cells). In addition, by fitting to the overall response exhibited by the cell in microbead twisting experiment, Fabry et al. [3] estimated the value of  $G_0$  to be  $\sim 41$  kPa for the reference frequency of  $\omega_0 \approx 25 \times 10^6$  rad/s, which scales to  $G_0 = 1.36$  kPa for  $\omega_0 = 1$  rad/s (assuming  $x = 1.2$  based on the experimental prediction), which is also in acceptable agreement with laser tracking microrheology observations in kidney epithelial cells [27].

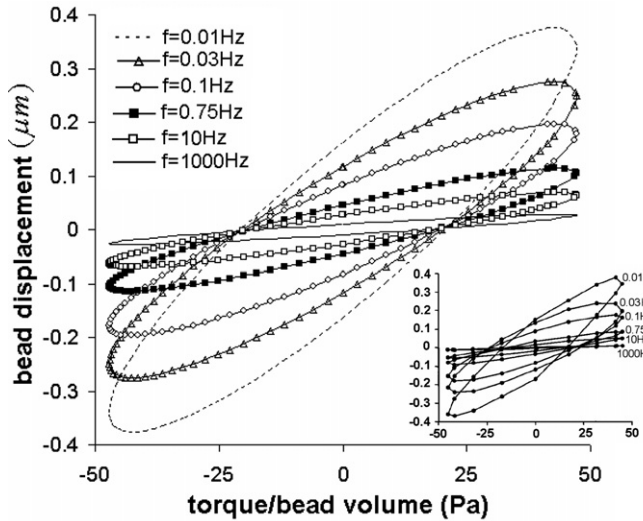


Fig. 4. Comparison between the numerical results and the experimental data from Fabry et al. for HASM cells [3] (inset). The average radius of the ferromagnetic microbeads used in the experiment and also the radius of the rigid sphere in the numerical simulations are  $2.25 \mu\text{m}$  with  $a/R = 0.178$ . Fitting to the experimental results yields the following material constants associated with power-law rheology:  $G_0 = 3.8 \text{ kPa}$  (for  $\omega_0 = 1 \text{ rad/s}$ ) and  $x = 1.3$  (corresponding to  $\eta \approx 0.51$ ). The following material parameters are used in the numerical simulations:  $\rho = 1 \text{ g/cm}^3$ ,  $E = 11 \text{ kPa}$  and  $\nu = 0.45$  (corresponding to  $K = 36.7 \text{ kPa}$ ). Results are presented for bead displacement vs. specific torque (the mechanical torque/bead volume).

It is noteworthy that the Newtonian viscosity term suggested by Fabry et al. [3] for justifying the curvilinearity observed in  $G''$  data at relatively high frequencies of excitation for most cell types is not incorporated in the results presented in Fig. 4. This added viscosity modifies the material shear loss modulus according to

$$G''(\omega) = \eta G'(\omega) + \mu\omega, \quad 1 \leq x < 2, \quad (8)$$

where  $\mu$  is the viscous damping coefficient and the storage modulus is that of Eq. (2). Here, the material loss modulus exhibits a higher degree of dependence on the excitation frequency with the exponent approaching 1 at very high frequencies, as observed experimentally. Fabry et al. [3] estimated that this additive viscosity, which is uncoupled from cytoskeleton dynamics, is on the order of  $1 \text{ Pa s}$ . A set of calculations was carried out to understand the role of this additive viscosity on the overall response of the material, Fig. 5. These calculations were performed at the excitation frequency of  $100 \text{ Hz}$  and for the following material parameters:  $\rho = 1 \text{ g/cm}^3$ ,  $E = 2.9 \text{ kPa}$ ,  $\nu = 0.45$ ,  $G_0 = 1 \text{ kPa}$  and  $\omega_0 = 1 \text{ rad/s}$ ,  $x = 1.2$ . As one would expect, this additive viscosity decreases the response amplitude at high frequencies of excitation, signaling the transition to fluid-like behavior. It is noteworthy that the frequency-domain viscosity model employed here is, in general, capable of modeling other frequency-dependant forms of microrheology. An additional example based on a new set of calculations is discussed in Fig. 6, where the structural damping coefficient of the material denoted by

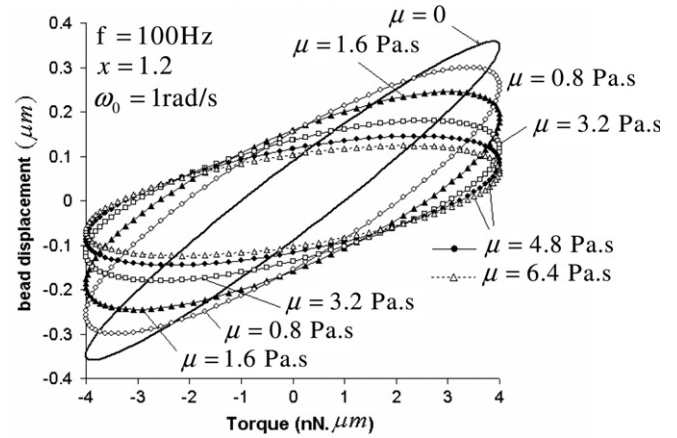


Fig. 5. Torque-displacement response in MTC at an excitation frequency of  $100 \text{ Hz}$  for various values of  $\mu$ . The shear loss modulus of the material follows Eq. (8). Calculations are performed for:  $G_0 = 1 \text{ kPa}$ ,  $\omega_0 = 1 \text{ rad/s}$ ,  $x = 1.2$ ,  $E = 2.9 \text{ kPa}$ ,  $\rho = 1 \text{ g/cm}^3$ ,  $\nu = 0.45$ . The rigid microbead has  $R = 2.25 \mu\text{m}$  with  $a/R = 0.178$ .

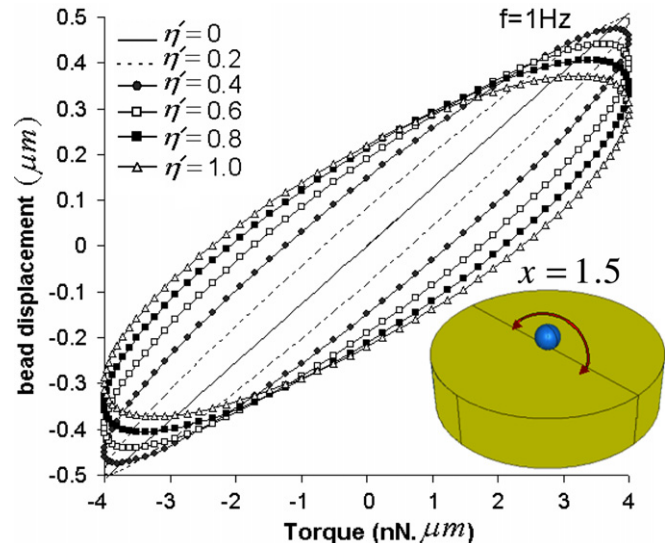


Fig. 6. In this set of calculations,  $G'(\omega) = G_0(\omega/\omega_0)^{x-1} \cos\left[\frac{(x-1)\pi}{2}\right]$  and  $G''(\omega) = \eta' G'(\omega)$ . Calculations are performed for:  $G_0 = 1.4 \text{ kPa}$ ,  $\omega_0 = 1 \text{ rad/s}$ ,  $E = 4 \text{ kPa}$ ,  $\rho = 1 \text{ g/cm}^3$ ,  $\nu = 0.45$ ,  $x = 1.5$ . The rigid microbead has a radius  $R = 2.25 \mu\text{m}$  with  $a/R = 0.178$ . Amplitude and frequency of the applied torque are  $4 \text{ nN } \mu\text{m}$  and  $1 \text{ Hz}$ , respectively.

$\eta'$  is taken as an independent material constant (note that the material law does not follow the power-law rheology).

### 6. Concluding remarks

A wide range of theoretical models exist for cytoskeletal mechanics, ranging from continuum models for cell deformation to actin filament-based models for cell motility [28]. A computational approach is presented here which incorporates the material model associated with power-law rheology observed in soft glassy materials when it is subjected to steady-state dynamic loading. The developed computational model is capable of relating the microrheology and

material constants to overall response of the material and is employed to model the cell response in microbead twisting cytometry to gain some insight into dynamics of cytoskeletal viscoelasticity under mechanical perturbation. Combination of the current computational model with rigorous experimental observations can provide a robust tool for investigating the rheology of cells and nuclei, providing insight into the complex dynamics of their response under mechanical stimuli.

### Acknowledgements

A.V. would like to thank Dr. David Weitz, Dr. Armand Ajdari and Dr. John W. Hutchinson for many insightful discussions. This work has been supported in part by the Division of Engineering and Applied Sciences, Harvard University (A.V., Z.X.) and in part by a grant (GM076689) from National Institutes of Health (R.D.K., M.R.K.M.).

### References

- [1] P. Sollich, Rheological constitutive equation for a model of soft glassy materials, *Phys. Rev. E* 58 (1998) 738–759.
- [2] B. Fabry, G.N. Maksym, J.P. Butler, M. Glogauer, D. Navajas, J.J. Fredberg, Scaling the microrheology of living cells, *Phys. Rev. Lett.* 87 (2001) 148102.
- [3] B. Fabry, G.N. Maksym, J.P. Butler, M. Glogauer, D. Navajas, N.A. Taback, E.J. Millet, J.J. Fredberg, Time scale and other invariants of integrative mechanical behavior in living cell, *Phys. Rev. E* 68 (4) (2003) 041914.
- [4] J. Alcaraz, L. Buscemi, M. Grabulosa, X. Trepast, B. Fabry, R. Farré, D. Navajas, Microrheology of human lung epithelial cells measured by atomic force microscopy, *Biophys. J.* 84 (2003) 2071–2079.
- [5] G. Lenormand, E. Millet, B. Fabry, J.P. Butler, J.J. Fredberg, Linearity and time-scale invariance of the creep function in living cells, *J. Roy. Soc. Interface* 1 (2004) 91–97.
- [6] N. Desprat, A. Richert, J. Simeon, A. Asnacios, Creep function of a single living cell, *Biophys. J.* 88 (2005) 2224–2233.
- [7] P. Bursac, G. Lenormand, B. Fabry, M. Oliver, D. Weitz, V. Viasnoff, J. Butler, J.J. Fredberg, Cytoskeletal remodeling and slow dynamics in the living cells, *Nat. Mater.* 4 (2005) 557–561.
- [8] B.D. Hoffman, G. Massiera, K.M. Van Citters, J.C. Crocker, The consensus mechanics of cultured mammalian cells, *Proc. Nat. Acad. Sci.* 103 (2006) 10259–10264.
- [9] M.L. Gardel, F. Nakamura, J.H. Hartwig, J.C. Crocker, T.P. Stossel, D.A. Weitz, Prestressed F-actin networks cross-linked by hinged filamins replicate mechanical properties of cells, *Proc. Nat. Acad. Sci.* 103 (2006) 1762–1767.
- [10] M. Puig-de-Morales, E. Millet, B. Fabry, D. Navajas, N. Wang, J.P. Butler, J.J. Fredberg, Cytoskeletal mechanics in adherent human airway smooth muscle cells: probe specificity and scaling of protein–protein dynamics, *Am. J. Physiol. Cell Physiol.* 287 (2004) C643–C654.
- [11] H. Gang, A.H. Krall, H.Z. Cummins, D.A. Weitz, Emulsion glasses: a dynamic light-scattering study, *Phys. Rev. E* 59 (1999) 715.
- [12] T.G. Mason, D.A. Weitz, Linear viscoelasticity of colloidal hard sphere suspensions near the glass transition, *Phys. Rev. Lett.* 75 (1995) 2770.
- [13] M. Cloitre, R. Borregam, L. Leibler, Rheological of aging and rejuvenation in microgel pastes, *Phys. Rev. Lett.* 85 (2000) 4819–4822.
- [14] M. Cloitre, R. Borregam, F. Monti, L. Leibler, Glassy dynamics and flow properties of soft colloidal pastes, *Phys. Rev. Lett.* 90 (2003) 68303.
- [15] E.R. Weeks, J.C. Crocker, A.C. Levitt, A. Schofield, D.A. Weitz, Three-dimensional direct imaging of structural relaxation near the colloidal glass transition, *Science* 287 (2000) 627–631.
- [16] P. Sollich, F. Lequeux, P. Hébraud, M.E. Cates, Rheology of soft glassy materials, *Phys. Rev. Lett.* 78 (1997) 2020.
- [17] D. Stamenovic, Z. Liang, J. Chen, N. Wang, Effect of the cytoskeletal prestress on the mechanical impedance of cultured airway smooth muscle cells, *J. Appl. Physiol.* 92 (2002) 1443–1450.
- [18] D. Stamenovic, B. Suki, B. Fabry, N. Wang, J.J. Fredberg, J.E. Buy, Rheology of airway smooth muscle cells is associated with cytoskeletal contractile stress, *J. Appl. Physiol.* 96 (2004) 1600–1605.
- [19] A.W.C. Lau, B.D. Hoffman, A. Davies, J.C. Crocker, T.C. Lubensky, Microrheology, stress fluctuations, and active behavior of living cells, *Phys. Rev. Lett.* 91 (2003) 198101.
- [20] ABAQUS User’s Manual, Version 6.0, Hibbit, Karlsson and Sorensen Inc., 2001.
- [21] S.M. Mijailovich, M. Kojic, M. Zivkovic, B. Fabry, J.J. Fredberg, A finite element model of cell deformation during magnetic bead twisting, *J. Appl. Physiol.* 93 (2002) 1429–1436.
- [22] H. Karcher, J. Lammerding, H. Huang, R.T. Lee, R.D. Kamm, M.R. Kaazempur-Mofrad, A three-dimensional viscoelastic model for cell deformation with experimental verification, *Biophys. J.* 85 (2003) 3336–3349.
- [23] A. Vaziri, H. Lee, M.R. Kaazempur-Mofrad, Deformation of the nucleus under indentation: mechanics and mechanisms, *J. Mater. Res.* 21 (2006) 2126–2135.
- [24] R.E. Laudadio, E.J. Millet, B. Fabry, S.S. An, J.P. Butler, J.J. Fredberg, Rat airway smooth muscle cell during actin modulation: rheology and glassy dynamics, *Am. J. Physiol. Cell Physiol.* 289 (2005) C1388–C1395.
- [25] N. Wang, J.P. Butler, D.E. Ingber, Mechanotransduction across the cell surface and through the cytoskeleton, *Science* 260 (1993) 1124–1127.
- [26] K.N. Dahl, A.J. Engler, J.D. Pajerowski, D.E. Discher, Power-law rheology of isolated nuclei with deformation mapping of nuclear substructures, *Biophys. J.* 98 (2005) 519–560.
- [27] S. Yamada, D. Wirtz, S.C. Kuo, Mechanics of living cells measured by laser tracking microrheology, *Biophys. J.* 78 (2000) 1736–1747.
- [28] M.R.K. Mofrad, R.D. Kamm (Eds.), *Cytoskeletal Mechanics: Models and Measurements*, Cambridge University Press, 2006.